*Tellus* (1989), *41A*, 200–208

# Transient-induced statistics in the atmosphere

By CARLO PELLACANI, SANDRO RAMBALDI, GIOVANNA SALUSTRI, *Department of Physics, University of Bologna, Via Irnerio 46, 40126 Bologna, Italy* and STEFANO SANTINI, *Department of Physics, University of Ancona, Piazza Roma 5, 60100 Ancona, Italy*

(Manuscript received 28 January 1987; in final form 10 June 1988)

ABSTRACT

The statistical effect of a time-changing zonal forcing on the large scale, barotropic components of the atmospheric circulation is considered. It is suggested that maxima of the statistical distribution of the zonal wind and traveling planetary wave intensity are the results of transitions between different, locally in time, dominating regimes. This interpretation is substantially different from that commonly adopted, which identifies the statistical maxima with the attractors of the theoretical models. To clarify this point, results from a numerical simulation, clearly showing the effects of transitions on distributions, are discussed. It is shown in particular how the properties of the basin of attraction of different regimes can deeply affect the resulting distributions of the relevant physical quantities. It is also shown how maxima of distributions have no simple connections with equilibria computed under the assumption of constant zonal forcing. These results suggest new interpretations of the statistics.

## 1. Introduction

After the introduction of low-order truncated models of the dynamic equations (Lorenz, 1963; Charney and De Vore, 1979) and others, researches on the statistical properties of large-scale atmospheric circulation were undertaken to verify such theories. Most of the work was devoted to the analysis of the low-frequency variability (time scales exceeding 10 days) that dominate the planetary flow patterns (Sawyer, 1970; Blackmon, 1976; Dole, 1982). The comparison between truncated spectral model predictions and statistical results were carried out comparing fixed stable points of the models with relative maxima of the statistical distribution of the real data; in other words, peaks of the statistical distributions were taken as representative of "equilibria" of the large-scale circulation (Charney et al., 1981; Reinhold and Pierrehumbert, 1982; Rambaldi and Mo, 1984; Speranza, 1986). Truncated models of large-scale atmospheric circulation are based on an arbitrary choice of eigenfunctions of some operator (often the Laplace operator) and most of the relevant predictions produced (attractors, stable equilibria, etc.) strongly depend on the choice of the number and the structure of the modes. We know that from the mathematical point of view, the convergence in some norm of the spectral series cannot be demonstrated for differential operators, such as those present in large-scale barotropic or baroclinic equations. Moreover, we know that in geophysical fluid dynamics, relevant features of the resulting truncated system, such as the nature of attractors and of bifurcations, depend on the chosen geometry (Lupini and Pellacani, 1984). The choice of the modes needs then to be based on some physical grounds, or on the capability of explaining some relevant observed feature. The analysis of meteorological data is rather difficult as far as the number of degrees of freedom is in fact infinite. The rôle of simple truncated models as theoretical guidance is very important as they can capture some relevant prototypes of non-linear phenomena in the atmosphere.

In this paper, we use a low-order truncated model of a barotropic, dissipative atmosphere with a varying (in time) zonal forcing to show

how the maxima of statistical distributions of zonal wind and wave amplitude are affected by a non-stationary zonal-forcing. It is found that the zonal wind distribution is essentially unimodal while the wave amplitude statistics exhibit a clear bimodality. Such features are then interpreted by showing that with a time-varying zonal forcing, different attractors globally dominate the dynamics in different time intervals. As the global attractiveness of different regimes can change abruptly when the non-stationary zonal forcing crosses critical values (see Section 2), the motion of the representative point in the phase space is deeply affected by such changes of the global attractor. The representative point starts moving toward the new attractor and the evolution of the system is dominated by the features of the basin of attraction quite far from the attractor itself. We show that the contributions of such transitions to the statistical distributions of zonal wind and wave amplitudes, are relevant.

The imposed oscillation of the zonal forcing (introduced to simulate the real variability of the zonal flow due to physical processes external to our model, such as baroclinic activity) is such that the two global attractors (an essentially zonal equilibrium and a periodic attractor with strong wave amplitudes) dominate the system in different parts of the period. In fact, the system is continuously approaching one of the attractors, but it never reaches it because the typical time of attractiveness of both attractors is significantly shorter than the time needed by the system to approach them.

In our analysis, the maxima of the statistical distributions are generated by the effects of the transitions between different regimes rather than by the regimes themselves. The effect is more evident for the zonal wind distribution which does not retain any information of the two equilibria alternatively dominating the phase space. Its only maximum does not correspond to any dominating zonal equilibrium.

The model discussed below is a simple prototype we use to show the rôle possibly played by the transitions on the statistics of the quantities involved. We consider a dissipative, three-mode, barotropic model with one zonal and two-wave components with a non-stationary forcing acting on the zonal flow only. The forcing is varied in time in different ways and the resulting statistics are considered and compared. It is shown that the most relevant features of the different distributions are similar and depend on the characteristics of the attraction basins of the attractors that become attractive during the forcing variations.

Further experiments have been carried out increasing the number (4 and 6) of spectral wave components according the selection rules. Qualitatively similar results have been obtained on the statistics for transitions between zonal fixed points, and for periodic oscillations with associated significant mean wave amplitudes, showing that in the limits of our experiments, the features of the statistical distributions are stable with respect to the introduction of new wave-like spectral components.

## 2. The basic theory

In this section, we briefly review the basic properties of the system of equations used in our analysis of the effects of transitions on the statistics. This system has been extensively studied (Lupini et al., 1983; Lupini and Pellacani, 1984). The truncated form of the two-dimensional non-divergent barotropic vorticity equation in spherical geometry for a forced dissipative flow can be written in the following form:

$$\dot{\zeta}_\alpha = 2(c_\beta - c_\gamma) k_\alpha \operatorname{Im}(\zeta_\beta \zeta_\gamma^*) - \nu_\alpha \zeta_\alpha + f_\alpha, \tag{2.1}$$

$$\dot{\zeta}_\beta = i(I_{\beta\beta\alpha} \zeta_\alpha + g_\beta) \zeta_\beta + i(c_\gamma - c_\alpha) k_\alpha \zeta_\alpha \zeta_\gamma - \nu_\beta \zeta_\beta, \tag{2.2}$$

$$\dot{\zeta}_\gamma = i(I_{\gamma\gamma\alpha} \zeta_\alpha + g_\gamma) \zeta_\gamma + i(c_\beta - c_\alpha) k_\alpha \zeta_\alpha \zeta_\beta - \nu_\gamma \zeta_\gamma, \tag{2.3}$$

where $\zeta_\beta$ and $\zeta_\gamma$ represent the complex amplitudes of the two wavelike spectral components we consider in our model, and $\zeta_\alpha$ is the amplitude of a zonal component interacting with the two waves. $\zeta_\alpha$ corresponds to a spherical harmonic $Y_\alpha^0$ with no longitudinal structure and $\zeta_\beta$ and $\zeta_\gamma$ to the spherical harmonics $Y_{n_\beta}^{l_\beta}$ and $Y_{n_\gamma}^{l_\gamma}$ with both latitudinal and longitudinal structure. Im means imaginary part, $\nu_\alpha$, $\nu_\beta$ and $\nu_\gamma$ are dissipation coefficients; $c_i$ and $g_i$ are structure parameters (Platzman, 1962; Lupini and Pellacani, 1984). For a given spherical harmonic $Y_p^j$, $j$ and $p$ are called longitudinal and latitudinal indexes. With the restriction $n_\gamma > n_\beta$ and $l_\beta = l_\gamma = l$, the interaction coefficients $I_{\beta\beta\alpha}$ and $I_{\gamma\gamma\alpha}$ satisfy well-known selection rules (Platzman, 1962):

$$I_{kk\alpha} \neq 0 \quad \text{for} \quad \alpha = 1, 3, \ldots, 2k-1. \tag{2.4}$$

$f_\alpha$ represents the forcing acting on the zonal flow component. The problem is simplified without losing important information if the following hypothesis is assumed for the dissipation coefficients acting on the wave components: $\nu_\alpha = \nu_\beta = \nu_\gamma = \bar{\nu}$.

In a previous paper (Lupini and Pellacani, 1984), henceforth referred to as "LP", the system of eqs. (2.1), (2.2) and (2.3) was studied for constant values of the zonal forcing. It was found that if the structure parameter $S$, defined by

$$S = (I_{\beta\beta\alpha} - I_{\gamma\gamma\alpha})^2 + 4(c_\beta - c_\alpha)(c_\gamma - c_\alpha)k_\alpha^2 \qquad (2.5)$$

satisfies the condition $S < 0$, two different globally attracting equilibria are found: if the forcing amplitudes belongs to the finite interval $(\nu_\alpha \zeta_\alpha^{(1)}, \nu_\alpha \zeta_\alpha^{(2)})$ where $\zeta_\alpha^{(1)}$ and $\zeta_\alpha^{(2)}$ are given by:

$$\zeta_\alpha^{(1,2)} = S^{-1}\{-\Delta g \Delta I \pm 2[(\Delta g^2 - 4\bar{\nu}^2) \times (c_\alpha - c_\gamma)k_\alpha^2 - \bar{\nu}^2 \Delta I^2]^{1/2}\} \qquad (2.6)$$

and $\Delta g = g_\beta - g_\gamma$ and $\Delta I = I_{\beta\beta\alpha} - I_{\gamma\gamma\alpha}$, then a stable, globally attracting zonal equilibrium dominates the phase space of the system. Outside this range, a forced periodic oscillation becomes the only attractor, with constant values of the waves amplitudes.

The case $S > 0$ has been considered (Lupini et al., 1983) (LPR hereafter) and is not discussed below as the bifurcation patterns for such triads are affected by the spherical geometry, and have no counterpart in truncated models in $\beta$-channels. For simplicity, we have concentrated on the more interesting case $S < 0$.

In the following, we will always refer to numerical and analytic results obtained for a zonal flow with meridional index 3 and for two waves with meridional indexes 2 and 4, and a longitudinal index 2. The angular velocity of the reference frame is taken to be 1, and the typical dissipation time is assumed to be of the order of 20 days ($\bar{\nu} = 0.05$). The results considered below can be applied, with attention, to all those cases where the selection rules and the condition $S < 0$ are satisfied. From a mathematical point of view, the quantity $f_\alpha$ acts as a bifurcation parameter; when it crosses one of the points given by eq. (2.6) from the interior of the interval, a new stable periodic solution appears and the zonal flow becomes unstable due to a supercritical Hopf bifurcation.

## 3. Transitions, a qualitative picture

As suggested in LPR, we can intuitively consider the effect of slow forcing variations, at least in the limit of almost adiabatic change: we imagine that the representative point in phase space asymptotically follows one of the attractors. When the forcing crosses the stability boundary, the point abruptly becomes attracted by the other attractor and starts moving towards it. The characteristics of the trajectories depend on the properties of the basin of attraction during this transition. There are some obvious consequences of this fact: first of all, if the basin of attraction is rather flat, then the approach speed of the representative point in phase space will be rather slow, and such a transition will have a relevant effect on the resulting statistics. Moreover, the structure of the basin of attraction does not depend on the particular time evolution of the zonal forcing, and is therefore, a stable property of a given model. Other numerical experiments, not shown here, suggest that the smoothness of the far basin of attraction of the zonal flow regimes is maintained in truncated models with more than 2 (4 and 6) spectral wave components, with almost identical effects on the statistical distributions of the amplitudes of waves and zonal flow components.

By numerical simulations (to be described in Section 4), it was found that the transitions from wave regime to zonal regime are characterized by a very slow motion of the representative point and therefore deeply affect the statistics, while the opposite transitions typically take place over a short time (of the order of 10 days) and do not play a relevant rôle in the statistics.

To properly understand the mechanism responsible for such basic features of our system, the almost adiabatic model can be adopted; two points are to be investigated, namely the location in phase space of the equilibria for the corresponding stationary model at a given time and their stability (or instability). Let us first notice that, by inspection of eqs. (2.1), (2.2) and (2.3) (see also LP), the wave regime equilibrium, when it exists, is stable and is characterized by a constant zonal component, corresponding to the critical value at which the Hopf bifurcation takes place. In Fig. 1, the heavy horizontal segment represents the locations of wave equilibria during

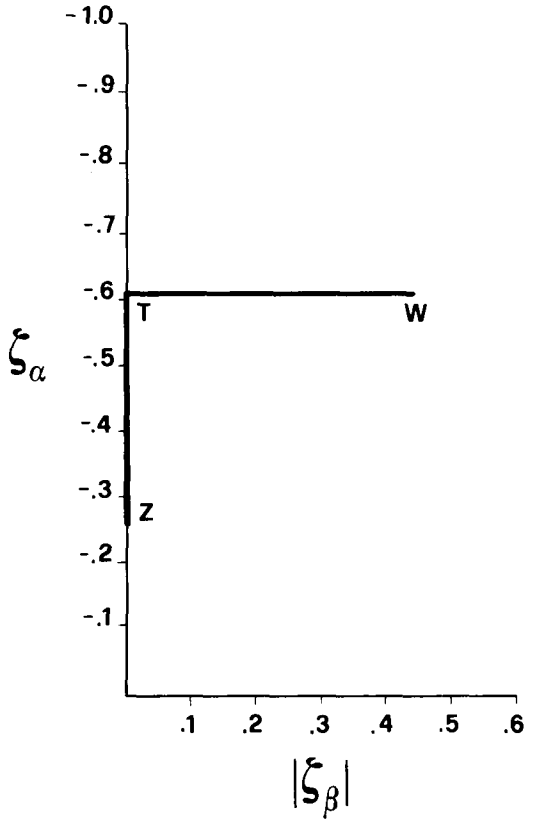


*Fig. 1.* Location of the stable equilibria with time-independent zonal forcing, for different amplitudes of the forcing. Increasing the forcing, the stable equilibrium moves from Z to T along the vertical solid segment and then from T toward W along the horizontal solid segment.

the part of the forcing oscillation when they exist; if they exist, they are stable, and the heavy vertical segment represents the locations of zonal equilibria, when stable, during the same oscillation. In the limit of the almost adiabatic analysis, there is always just one stable attracting point at a given time of the oscillation; such an attractor moves along the trajectory represented by the two segments described above. The attractor moves, during a period of the forcing from Z to T along the vertical segment and from T to W along the horizontal segment; then it reverses the direction of its motion following the same path.

By inspection of Fig. 4, we are left with the problem of interpreting the upper portion of the trajectory where the representative point still moves toward zonal regimes with higher values of zonal wind intensity that do not correspond to any attracting equilibria during the forcing period (all the equilibria stay on the couple of segments Z–T and T–W).

Let us briefly review what is observed in numerical simulations as those of Fig. 4. When the attractor is in the lower part of the vertical segment (near to the point Z), the representative point is not far from it, and once the equilibrium has reached its extremum at Z and reverses its motion, the point starts following it. When the point T is reached, no more attracting zonal equilibria exist and the only attractor of the system is the wave-like one which moves, increasing the forcing, from T to W. The representative point of the truncated system nevertheless continues its motion along the vertical axis and only after a considerable time interval does it leave the region of zonal regimes and rapidly moves toward the attracting wavy regime. For forcing periods of the order of those considered in this paper, the representative point sits, after some oscillations, in such a regime and follows it. This typically happens after the equilibrium has reached its maximum at point W and has inverted the direction of its motion. Following that, the representative point then follows the moving (because of the varying forcing) equilibrium, until it disappears at point T. After that, the representative point is attracted by the zonal equilibrium and moves downward.

The two transitions are thus essentially different in their physical nature: during the lower transition, the representative point slowly moves toward zonal equilibria essentially following the evolution in time of the attracting wave regime. The upper transition takes place from unstable zonal regimes, and this happens rapidly. To understand this last feature, a local stability analysis of the attracting regimes, alternating during the period of the forcing oscillation, is to be considered. Referring again to the case of Fig. 4, it is observed that, when it exists (T–W in the figure), the wave-like equilibrium is locally stable, with one real and two complex conjugate eigenvalues. The real parts of such eigenvalues are small and exactly of the order of the dissipation time.

For the zonal equilibria, the local stability analysis shows that in its stability range (Z–T in

Table 1. *Eigenvalues (days$^{-1}$) of the linear stability problem for the zonal equilibrium; $\mathrm{Re}(\lambda) < 0$ indicates stable modes*

| | $\lambda_1$ | | $\lambda_2$ | | $\lambda_3$ | |
|---|---|---|---|---|---|---|
| $\zeta_a$ | Re | Im | Re | Im | Re | Im |
| −1.000 | 0.235 | −1.338 | −0.335 | −1.338 | −0.050 | 0.000 |
| −0.960 | 0.217 | −1.347 | −0.317 | −1.347 | −0.050 | 0.000 |
| −0.920 | 0.199 | −1.356 | −0.299 | −1.356 | −0.050 | 0.000 |
| −0.880 | 0.180 | −1.366 | −0.280 | −1.366 | −0.050 | 0.000 |
| −0.840 | 0.160 | −1.375 | −0.260 | −1.375 | −0.050 | 0.000 |
| −0.800 | 0.138 | −1.384 | −0.238 | −1.384 | −0.050 | 0.000 |
| −0.760 | 0.116 | −1.393 | −0.216 | −1.393 | −0.050 | 0.000 |
| −0.720 | 0.090 | −1.402 | −0.190 | −1.402 | −0.050 | 0.000 |
| −0.680 | 0.061 | −1.411 | −0.161 | −1.411 | −0.050 | 0.000 |
| −0.640 | 0.024 | −1.420 | −0.124 | −1.420 | −0.050 | 0.000 |
| −0.600 | −0.050 | −1.396 | −0.050 | −1.463 | −0.050 | 0.000 |
| −0.560 | −0.050 | −1.353 | −0.050 | −1.524 | −0.050 | 0.000 |
| −0.520 | −0.050 | −1.333 | −0.050 | −1.562 | −0.050 | 0.000 |
| −0.480 | −0.050 | −1.321 | −0.050 | −1.593 | −0.050 | 0.000 |
| −0.440 | −0.050 | −1.313 | −0.050 | −1.620 | −0.050 | 0.000 |
| −0.400 | −0.050 | −1.307 | −0.050 | −1.643 | −0.050 | 0.000 |
| −0.360 | −0.050 | −1.304 | −0.050 | −1.665 | −0.050 | 0.000 |
| −0.320 | −0.050 | −1.302 | −0.050 | −1.685 | −0.050 | 0.000 |
| −0.280 | −0.050 | −1.303 | −0.050 | −1.703 | −0.050 | 0.000 |

Fig. 1), the two complex conjugate eigenvalues are again characterized by negative real parts exactly of the order of the dissipation time. After the critical value of forcing is crossed, one of the eigenvalues obviously exhibits a positive real part that rapidly grows with the forcing amplitude.

We can then try to explain why, once point T is reached, the representative point continues its motion towards higher values of essentially zonal regimes. By numerical evaluation of the eigenvalues, it is seen (Tables 1, 2) that the wave-like regime is in fact locally attractive, but the very small values of the negative real part of its eigenvalues suggest a very weak attractive effect in phase space. It is thus the instability of the zonal regime rather than the attractiveness of the wave regime that is responsible for the rapid upper transition of Fig. 4. In fact, after the Hopf bifurcation, i.e., for zonal regimes corresponding to zonal flows above point T of Fig. 1, such an unstable fixed point is characterized by increasing (with the forcing) positive real parts of its eigenvalues. The representative point of the system then remains near to the unstable equilibrium, as it feels a very weak attraction effect through the stable wave equilibrium, until it is shot away by the increasing instability of the zonal regime itself. In Tables 1, 2, the eigenvalues of the zonal and wave-like regimes are listed for different values of the zonal forcing, respectively. We are thus in a position to clearly understand the essential physical difference between the two transitions: referring again to Fig. 4, it is seen that the lower transition takes place with the typical time of the forcing variation. The upper transition, from the zonal to the wave-like regime, in contrast is characterized by the typical time of instability of the unstable zonal flow regime. Thus, the basic mechanism responsible for the statistical features observed in the numerical simulations reported in Section 4 is the permanence of the representative point of the system near the zonal equilibrium, even in a period of the forcing cycle when the zonal flow is not a stable equilibrium and the other wave-like equilibrium is very weak. This effect is maintained when more than two wave-like components are considered, and then seems to be a rather general effect for an atmosphere such as that considered in our model characterized by an oscillating zonal forcing.

Table 2. *Eigenvalues (days$^{-1}$) of the linear stability problem for the wavy equilibrium; $\mathrm{Re}(\lambda) < 0$ indicates stable modes*

| | $\lambda_1$ | | $\lambda_2$ | | $\lambda_3$ | |
|---|---|---|---|---|---|---|
| $f_\alpha$ | Re | Im | Re | Im | Re | Im |
| −0.0314 | −0.025 | 0.019 | −0.025 | −0.019 | −0.100 | 0.000 |
| −0.0323 | −0.025 | 0.059 | −0.025 | −0.059 | −0.100 | 0.000 |
| −0.0333 | −0.025 | 0.081 | −0.025 | −0.081 | −0.100 | 0.000 |
| −0.0342 | −0.025 | −0.098 | −0.025 | 0.098 | −0.100 | 0.000 |
| −0.0351 | −0.025 | −0.112 | −0.025 | 0.112 | −0.100 | 0.000 |
| −0.0361 | −0.025 | 0.125 | −0.025 | −0.125 | −0.100 | 0.000 |
| −0.0370 | −0.025 | −0.137 | −0.025 | 0.137 | −0.100 | 0.000 |
| −0.0379 | −0.025 | −0.148 | −0.025 | 0.148 | −0.100 | 0.000 |
| −0.0389 | −0.025 | −0.158 | −0.025 | 0.158 | −0.100 | 0.000 |
| −0.0398 | −0.025 | 0.167 | −0.025 | −0.167 | −0.100 | 0.000 |
| −0.0407 | −0.025 | −0.176 | −0.025 | 0.176 | −0.100 | 0.000 |
| −0.0417 | −0.025 | 0.185 | −0.025 | −0.185 | −0.100 | 0.000 |
| −0.0426 | −0.025 | −0.193 | −0.025 | 0.193 | −0.100 | 0.000 |
| −0.0435 | −0.025 | 0.201 | −0.025 | −0.201 | −0.100 | 0.000 |
| −0.0445 | −0.025 | 0.208 | −0.025 | −0.208 | −0.100 | 0.000 |
| −0.0454 | −0.025 | −0.216 | −0.025 | 0.216 | −0.100 | 0.000 |
| −0.0463 | −0.025 | 0.223 | −0.025 | −0.223 | −0.100 | 0.000 |
| −0.0473 | −0.025 | 0.229 | −0.025 | −0.229 | −0.100 | 0.000 |
| −0.0482 | −0.025 | −0.236 | −0.025 | 0.236 | −0.100 | 0.000 |
| −0.0491 | −0.025 | −0.242 | −0.025 | 0.242 | −0.100 | 0.000 |
| −0.0501 | −0.025 | −0.249 | −0.025 | 0.249 | −0.100 | 0.000 |
| −0.0510 | −0.025 | −0.255 | −0.025 | 0.255 | −0.100 | 0.000 |
| −0.0519 | −0.025 | −0.261 | −0.025 | 0.261 | −0.100 | 0.000 |
| −0.0529 | −0.025 | −0.266 | −0.025 | 0.266 | −0.100 | 0.000 |
| −0.0538 | −0.025 | 0.272 | −0.025 | −0.272 | −0.100 | 0.000 |
| −0.0547 | −0.025 | 0.278 | −0.025 | −0.278 | −0.100 | 0.000 |

## 4. Numerical simulations

In order to simulate a realistic variation of the forcing parameter, with several time scales, numerical experiments were performed with a forcing function in the form:

$$f(t) = f_0\left(1 + \sum_{n=1} a_n \sin\left(\frac{t}{T_n} + \phi_n\right)\right), \qquad (4.1)$$

representing a superposition of different oscillations with periods $T_n/2\pi$. All the simulations were performed with a fourth-order Runge–Kutta numerical scheme with a time-step of 0.1 days. We considered $T_n$ equal 10, 15, 20, 30, 40, 50, 100, 150, 200 and 250 days respectively, with random initial phases. We ran several experiments. The model was integrated for a long interval (20,000 days) and the distribution of the amplitude of the zonal flow and the amplitude of the wave components $|\zeta_\beta|$ were computed.

In a first experiment, we considered a single oscillating component with a period of 188 days. The forcing function is given by

$$f(t) = -0.0314(1 + 0.7 \sin(t/30)), \qquad (4.2)$$

where we choose $f_0 = -0.0314$ because this is a critical value for which the Hopf bifurcation takes place. The statistics produced by this experiment are shown in Figs. 2, 3. The effect of the transition dynamics on the distribution of $|\zeta_\alpha|$ is evident: the maximum between 0.4 and 0.5 cannot be explained in terms of the existence of a zonal attractor in this interval, during the cycle of the forcing function. In Fig. 4, a sketch of the trajectory in phase space of the test experiment is given: statistical analysis and direct observations of the model evolutions show that the maximum in the distribution of $|\zeta_\alpha|$ in Fig. 3 is due to the section (A, B) of the trajectory, which corresponds to the transition from the wave-like

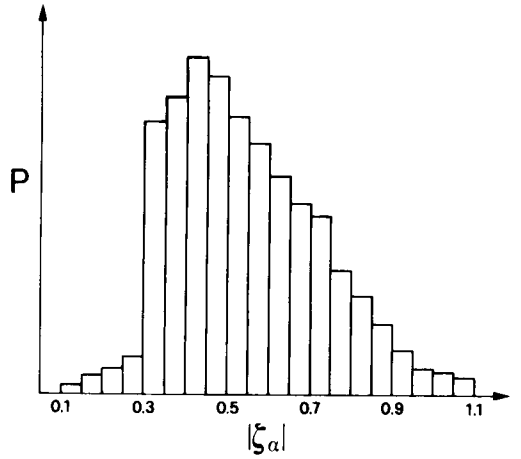


*Fig. 2.* Normalized probability distribution $P$ of the zonal component amplitude for a zonal forcing given by: $f(t) = -0.0314(1 + 0.7 \sin(t/30))$. The simulation time is 20,000 days.

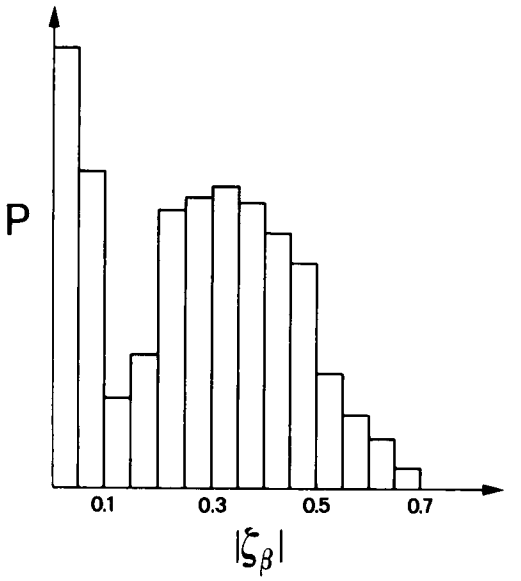


*Fig. 3.* Normalized probability distribution $P$ of the wave amplitude for a zonal forcing given by: $f(t) = -0.0314(1 + 0.7 \sin(t/30))$. The simulation time is 20,000 days.

regime to the zonal regime. The transition is extremely slow and the system spends almost 35% of the forcing period performing it. The opposite transition (C, D) in Fig. 4 is quite rapid, of the order of 5% of the forcing period. We then conclude that the maximum of the distribution of Fig. 2 is due to the slow nature of the transition

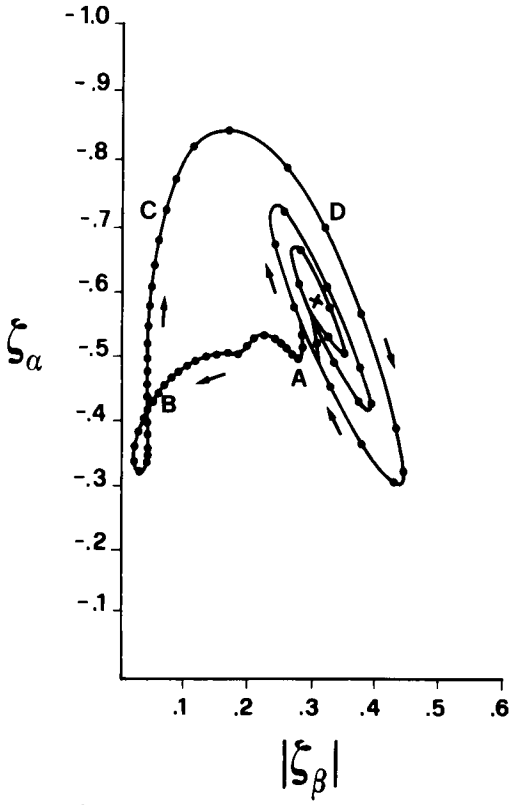


*Fig. 4.* Sketch of the trajectory of the representative point with a zonal forcing given by: $f(t) = -0.0314(1 + 0.7 \sin(t/30))$. The wavy regime is indicated with a cross. While the representative point moves along the trajectory from A to C, the corresponding zonal equilibrium lies on the $|\zeta_\beta| = 0$ axis, with values of $\zeta_\alpha$ ranging from $-0.3$ to $-0.7$.

from wave regime to the zonal regime. Fig. 3 shows how the maxima in the wave component amplitude still retains some information on the two equilibria present in the corresponding case with constant forcing, while this information is absent in the statistics of zonal flow. Because of its essential asymmetry with respect to the minimum, such a distribution must not be confused with that generated by a single standing wave. In the light of the results of this test experiment, we analyse the numerical results obtained by simulating more complex time-varying zonal forcings. In a second experiment, we add another component in the forcing:

$$f(t) = -0.0314(1 + 0.7 \sin(t/30) + 0.2 \sin(t/8)). \quad (4.3)$$

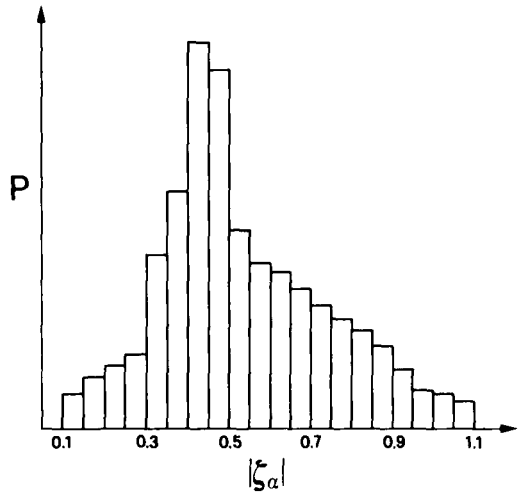


*Fig. 5.* Normalized probability distribution $P$ of the zonal component amplitude for a zonal forcing given by: $f(t) = -0.0314(1 + 0.7\sin(t/30) + 0.2\sin(t/8))$. The simulation time is 20,000 days.

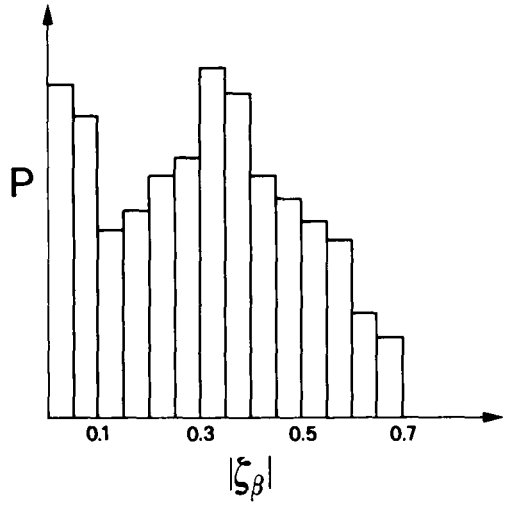


*Fig. 6.* Normalized probability distribution $P$ of the wave amplitude for a zonal forcing given by: $f(t) = -0.0314(1 + 0.7\sin(t/30) + 0.2\sin(t/8))$. The simulation time is 20,000 days.

The statistical distributions again obtained by long-time integrations came out very similar to the previous case and are not included here. In a third experiment, we run the model with different values of the amplitudes $a_n$ of the periodic components. In particular, we consider a maximum at $T_n = 30$ days ($a_{T_n=30} = 0.7$) and we set $a_n/a_{T_n=30} = 0.1$ for all the other oscillating

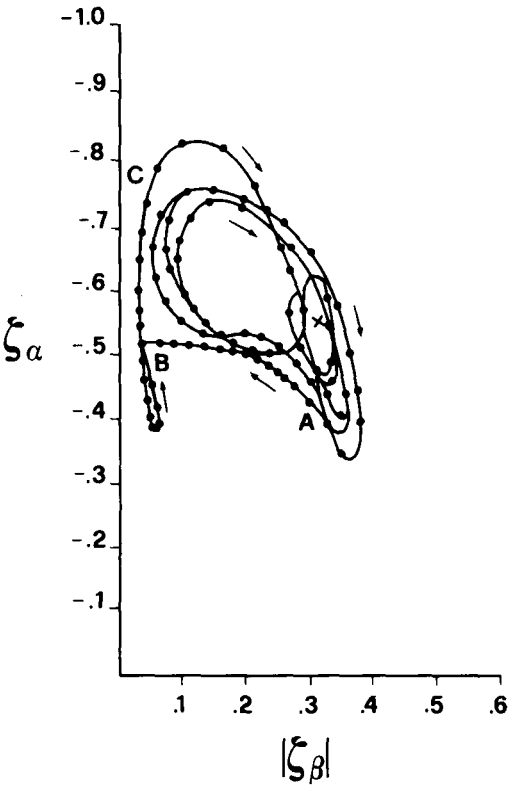


*Fig. 7.* Sketch of the trajectory of the representative point with a zonal forcing given by: $f(t) = -0.0314(1 + 0.7\sin(t/30) + 0.2\sin(t/8))$. The wavy regime is indicated with a cross. While the representative point moves along the trajectory from A to C, the corresponding zonal equilibrium lies on the $|\zeta_\beta| = 0$ axis, with values of $\zeta_\alpha$ ranging from $-0.3$ to $-0.7$.

components, thus simulating a maximum of the forcing activity for the period $T = 188$ days. Figs. 5 and 6 shows the statistics worked out by such simulations and Fig. 7 shows a sketch of the trajectory in phase space in this experiment. We first observe that no relevant differences are found for the two new spectra (maximum at low frequencies or at $T = 30$ days). The fundamental features observed in the case of Figs. 2, 3 are retained: the zonal flow distributions exhibit a single maximum that corresponds to the transition from the wave regime to the zonal regime: the peak is now more spread. However, this seems the only difference between this case and the test experiment. By inspection of Fig. 6, it is seen that the same two maxima of the test case

are also obtained for very complicated time dependences of the forcing function. The two maxima are slightly more spread, but the gap between the two is still relevant and is reproduced independently of the choices of the hystogram step. As manifest in LPR, the spreading of maxima is essentially due to the presence of a large number of forcing frequencies, that induces a very complicated spectrum on the zonal component because of the essential non-linearity of our system. The wave-like components, on the other hand, do not exhibit a significant non-linear spreading of their spectrum (see again LPR).

## 5. Concluding remarks

Introducing the concept of multiple equilibria in large-scale circulation, Charney and deVore (1979) suggested that the atmosphere possesses several equilibrium regimes. They also suggested that that which is responsible for the transitions from one equilibrium to another, might be the small-scale synoptic instabilities (Gall et al., 1979; Sanders ad Gyakum, 1980).

In this paper, we have tested the possibility that, rather than oscillating between multiple stationary equilibria obtained by a fixed value of the forcing zonal parameter, the large-scale, barotropic components of the atmosphere feels dynamically significant variations in time of the forcing itself, causing the local-in-time dominance of different attracting regimes. Results considered in the previous section show how a simple truncated model of a barotropic, dissipative atmosphere under the action of a time-varying zonal forcing, generates statistics whose connection with the attractors, present in the cases of constant forcings, is more complicated than what might be thought in a simple, intuitive analysis. In particular, we have shown the effects of what we have called "transitions", i.e., those time intervals when the representative point in phase space feels the abrupt disappearance of the wave-like attractor and starts to move slowly toward a zonal configuration. It was shown that during this stage, the representative point moves in the far basin of attraction of the zonal flow, whose characteristics are not captured by local stability analysis of the equilibrium.

## 6. Acknowledgements

The authors were supported in part by MPI grants, and by the Italian CNR grants.

## REFERENCES

Blackmon, M. I. 1976. A climatological spectral study of the 500 mb geopotential height in the northern hemisphere. *J. Atmos. Sci. 33*, 1607–1623.

Charney, J. G. and DeVore, J. G. 1979. Multiple flow equilibria in the Atmosphere and Blocking. *J. Atmos. Sci. 36*, 1205–1216.

Charney, J. G., Shukla, J. and Mo, K. C. 1981. Comparison of a barotropic blocking theory with observation. *J. Atmos. Sci. 38*, 762–779.

Dole, R. M. 1982. Persistent anomalies of the extratropical northern hemisphere wintertime circulation. Ph.D. thesis, Massachusetts Institute of Technology, USA.

Gall, R. R., Blakeslee, R. and Somerville, R. J. C. 1979. Cyclone scale forcing of ultralong waves. *J. Atmos. Sci. 30*, 1040–1053.

Lorenz, E. N. 1963. Deterministic nonperiodic flow. *J. Atmos. Sci. 20*, 130–141.

Lupini, R., Pellacani, C. and Rambaldi, S. 1983. Truncated model of a barotropic atmosphere with a periodic forcing. *Pageoph 121*, 1003–1017.

Lupini, R. and Pellacani, C. 1984. On forced and unforced triadic models of atmospheric flows. *Tellus 36A*, 11–20.

Platzman, G. W. 1962. The analytical dynamics of the spectral vorticity equation. *J. Atmos. Sci. 19*, 313–332.

Rambaldi, S. and Mo, K. C. 1984. Forced stationary solutions in a barotropic channel: Multiple equilibria and theory of non linear resonance. *J. Atmos. Sci. 41*, 3135–3146.

Reinhold, B. B. and Pierrehumbert, R. T. 1982. Dy-nam-ics of weather regimes: Quasi stationary waves and blocking. *Mon. Weather Rev. 110*, 1105–1145.

Sanders, F. and Gyakum, J. 1980. Synoptic dynamic climatology of the bomb. *Month. Weath. Rev. 108*, 1589–1606.

Sawyer, J. S. 1970. Observational characteristics of fluctuations with a time scale of a month. *Quart. J. Roy. Met. Soc. 96*, 610–625.

Speranza, A. 1986. Deterministic and statistical properties of northern hemisphere, middle latitude circulation: minimal theoretical models. *Advances in Geophysics 29*, 150–192.